High Kinetic Stability of HXeBr upon Interaction with Carbon Dioxide: HXeBr···CO 2 Complex in a Xenon Matrix and HXeBr in a Carbon Dioxide Matrix

ARTICLE *in* THE JOURNAL OF PHYSICAL CHEMISTRY A · APRIL 2012

Impact Factor: 2.69 · DOI: 10.1021/jp301704n · Source: PubMed

6 AUTHORS, INCLUDING:

Masashi Tsuge
National Chiao Tung University
21 PUBLICATIONS **119** CITATIONS
SEE PROFILE

Markku Rasanen
University of Helsinki
267 PUBLICATIONS **7,025** CITATIONS
SEE PROFILE

THE JOURNAL OF PHYSICAL CHEMISTRY A

Article

pubs.acs.org/JPCA

High Kinetic Stability of HXeBr upon Interaction with Carbon Dioxide: HXeBr···CO_2 Complex in a Xenon Matrix and HXeBr in a Carbon Dioxide Matrix

Masashi Tsuge,[†] Slawomir Berski,[‡] Radoslaw Stachowski,[‡,§] Markku Räsänen,[†] Zdzislaw Latajka,[‡] and Leonid Khriachtchev*[,†]

[†]Department of Chemistry, University of Helsinki, P.O. Box 55, FIN-00014, Finland

[‡]Faculty of Chemistry, University of Wroclaw, 14, F. Joliot-Curie Str., 50-383 Wroclaw, Poland

[§]Wroclaw Centre for Networking and Supercomputing, HPC Department, Technical University, pl. Grunwaldzki 9, bud. D2/101, 50-337 Wroclaw, Poland

Supporting Information

ABSTRACT: We investigate the conditions when noble-gas hydrides can be found in real environments and report on the preparation and identification of the HXeBr···CO_2 complex in a xenon matrix and HXeBr in a carbon dioxide matrix. The H−Xe stretching mode of the HXeBr···CO_2 complex in a xenon matrix is observed at 1557 cm^{-1}, showing a spectral shift of +53 cm^{-1} from the HXeBr monomer. The calculations at the CCSD(T)/aug-cc-pVTZ-PP(Xe,Br) level of theory give two stable structures for the HXeBr···CO_2 complex with frequency shifts of +55 and +103 cm^{-1}, respectively. On the basis of the calculations, the experimentally observed band is assigned to the more stable structure with a "parallel" geometry. The HXeBr molecule was prepared in a carbon dioxide matrix and has the H−Xe stretching frequency of 1646 cm^{-1}, meaning a strong matrix shift and stabilization of the H−Xe bond. The deuterated species DXeBr in a carbon dioxide matrix absorbs at 1200 cm^{-1}. This is the first case where a noble-gas hydride is prepared in a molecular solid. The thermal stabilities of HXeBr and HXeBr···CO_2 complex in a xenon matrix and HXeBr in a carbon dioxide matrix were examined. We have found a high thermal stability of HXeBr in carbon dioxide ice (at least up to 100 K), i.e., under conditions that may occur in nature.

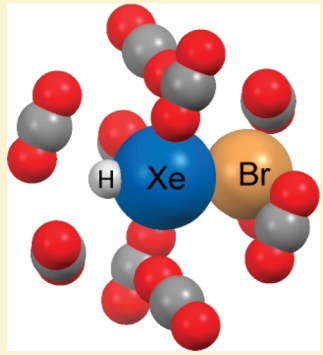

INTRODUCTION

Noble-gas hydrides with general formula HNgY (Ng = a noble-gas atom and Y = an electronegative group) form a part of modern noble-gas chemistry.[1,2] Since the first discovery in 1995,[3] 26 noble-gas hydrides have been reported including the argon compound $HArF$[4,5] and the most recent addition of HXeOBr.[6] The noble-gas hydrides can be prepared by photolysis of an HY precursor and subsequent thermal mobilization of H atoms in a noble-gas matrix, which leads to the reaction H + Ng + Y → HNgY. The HNgY molecules are characterized by an ion-pair $(HNg)^+Y^-$ nature and strong intensity (~1000 km mol^{-1}) of the H−Ng stretching vibration, which allows one to easily detect them by IR spectroscopy.

Because the HNgY molecules are weakly bound and have a large dipole moment, interaction with other molecules and matrix has a pronounced effect on their vibrational properties. These systems have attracted both theoretical and experimental attention.[7−10] The experimentally observed HNgY complexes to date are $HArF···N_2$, $HKrF···N_2$, $HKrCl···N_2$, HKrCl···HCl, $HXeBr···N_2$, $HXeCl···N_2$, HXeBr···HBr, HXeBr···HCl, HXeCl···HCl, $HXeCCH···CO_2$, HXeCCH···HCCH, and $HXeOH···H_2O$.[11−18] The number of calculated systems is much bigger. One important finding on these species is the blue shift of the H−Ng stretching vibration observed upon complexation,[8] which indicates a stabilization of this chemical bond. The H−Xe stretching frequency shifts in the HXeY···HX (X, Y = Cl or Br) complexes can exceed +100 cm^{-1}.[15] The HKrCl···HCl complex shows a huge blue shift of ca. +300 cm^{-1}, which is probably the largest blue shift upon the 1:1 complex formation.[13] The blue shifts have been observed not only for bonding to the H−Ng part but also without hydrogen bonding. The blue shift of the H−Xe stretching mode is a normal effect for noble-gas hydrides, and it has been attributed to the enhanced ion-pair character. This is in contrast to most of the hydrogen-bonded systems A···H−X (A and H−X are hydrogen acceptor and donor species, respectively) where the H−X stretching frequency usually red-shifts.

The noble-gas hydrides, which have been prepared experimentally, are practically absolutely stable at low matrix temperatures (~10 K). However, it has been shown that some of these species decompose in matrices at elevated temperatures. In particular, HXeOH was found to decompose in a xenon matrix at 54 K.[19] Two decomposition channels have been discussed:[1]

Received: February 21, 2012
Revised: April 11, 2012
Published: April 11, 2012

   dx.doi.org/10.1021/jp301704n | J. Phys. Chem. A 2012, 116, 4510−4517

$$HNgY \rightarrow Ng + HY \quad (1)$$

$$HNgY \rightarrow H + Ng + Y \quad (2)$$

The first reaction, referred to as the two body (2B) channel, is always highly exoergic, but the bending barrier is sufficient to ensure the kinetic stability of HNgY molecules at low temperatures. The second reaction is referred to as the three body (3B) channel via the stretching coordinate. The theoretical studies suggest that the thermal stability of HNgY molecules is mainly controlled by the 3B channel.[1] HXeCCH is theoretically predicted to have a half-life of 3 h at 0 °C and to be practically stable under −20 °C.[20] It is also important to know whether the complex formation affects the kinetic stability of HNgY. The molecular dynamics simulations by Tsivion and Gerber show that HXeCCH in acetylene clusters may be chemically stable up to 150 K.[21]

The energetic stabilization or destabilization of HNgY molecules by a matrix is experimentally a fully open question, and its theoretical description is also lacking. Khriachtchev et al. studied the relative stability of HXeOH and HXeOXeH at 55 K,[22] and the results were in complete disagreement with the theoretical predictions.[23] One can speculate that the calculations are done for the species in vacuum whereas the experiment is performed in the solid phase. It is known that the H−Ng stretching frequency depends largely on the noble-gas matrix. For example, the H−Xe stretching frequencies of HXeBr are 1504, 1524, and 1452.5 cm^{-1} in xenon, krypton, and neon matrices, respectively.[3,24] If the kinetic stability of these molecules is somehow connected with the strength of the H−Ng bond, the HNgY stability may change accordingly. From this viewpoint, it is interesting to prepare HNgY molecules in molecular matrices that should have a stronger solvation effect compared to noble-gas matrices. A carbon dioxide matrix is an attractive candidate for this study because this solid can be annealed at relatively high temperatures. Chemistry in solid carbon dioxide is attracting a lot of attention because of its important role as the chemical inventory of the regions of star and planet formation.[25]

In the present work, we inspect interaction of HXeBr, one of the most studied noble-gas hydride, with carbon dioxide. We report the HXeBr···CO_2 complex in a xenon matrix and HXeBr in a carbon dioxide matrix. These species are identified using IR absorption spectroscopy. The HXeBr···CO_2 complex in a xenon matrix is assigned with the aid of quantum chemical calculations. The preparation of HXeBr in a carbon dioxide matrix is the first case of a noble-gas hydride in a molecular matrix. We compare the thermal stability of HXeBr monomer and HXeBr···CO_2 complex in a xenon matrix and HXeBr monomer in a carbon dioxide matrix. Our main motivation is to find a stabilization effect of carbon dioxide on HXeBr, and the positive result is obtained.

COMPUTATIONAL DETAILS AND RESULTS

The calculations are performed using the CCSD(T),[26] MP2(full),[27] and DFT(B3LYP)[28−30] methods. The aug-cc-pVTZ and aug-cc-pVQZ basis sets[31,32] are obtained from the EMSL Basis Set Library using the Basis Set Exchange software.[33,34] For the Br and Xe atoms, 10 and 28 electrons, respectively, are described by pseudopotentials. The minima on the potential energy surface are verified on the basis of the harmonic vibrational analysis, which yields no imaginary frequencies. The interaction energy is obtained as the difference of the total energies of the complex and HXeBr and CO_2 monomers (with the structures in the complex) corrected for the basis set superposition error (BSSE) using the counterpoise procedure.[35] The charge distributions are obtained with the natural population analysis (NPA) method.[36] The calculations of the geometries and relative energies at the CCSD(T)/aug-cc-pVTZ-PP level are performed with the MOLPRO program[37] and at the other levels of theory with the Gaussian 09 program.[38] The interaction energies at the CCSD(T) level are calculated using the Gaussian 09 program.

Two minima on the potential energy surface of the HXeBr···CO_2 complex are found (Figure 1). The parallel complex is presumably stabilized by dispersion forces, and the linear complex is stabilized by the O···H−Xe hydrogen bond. Upon the formation of the complexes, the most substantial change is observed for HXeBr: the H−Xe bond shortens by 0.012−0.013 Å, and the Xe−Br bond elongates by a very similar value whereas the structural change is much smaller for the CO_2 molecule. The partial atomic charges are shown in Table 1. Upon complex formation, the positive charge of the (HXe) part increases, with this increase being somewhat greater for the linear complex.

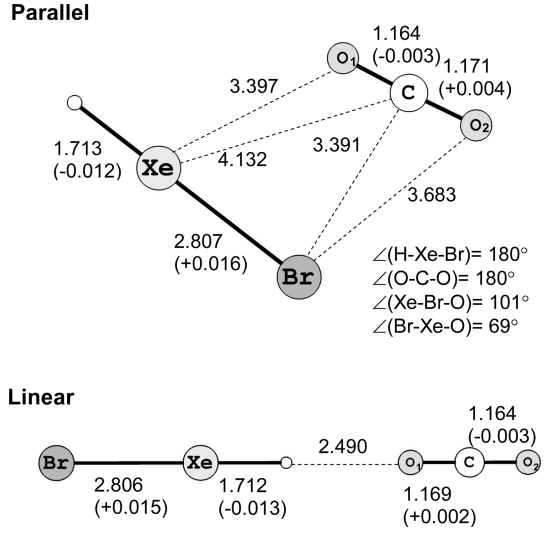

Figure 1. Structures of the parallel and linear HXeBr···CO_2 complexes optimized at the CCSD(T)/aug-cc-pVTZ-PP level of theory. The bond lengths are in angstroms. The values in parentheses show the effect of the complex formation relative to the HXeBr and CO_2 monomers optimized at the same level of theory.

Table 1. Partial Atomic Charges (in Elementary Charges) for the Parallel and Linear Complexes Calculated at the CCSD/aug-cc-pVTZ-PP//CCSD(T)/aug-cc-pVTZ-PP Level of Theory Using the Natural Population Analysis (NPA)

		HXeBr···CO_2 complexes	
	monomers HXeBr, CO_2	parallel	linear
q(H)	−0.026	−0.012	+0.001
q(Xe)	+0.656	+0.670	+0.658
q(Br)	−0.630	−0.653	−0.661
q(C)	+1.006	+1.026	+1.017
q(O1)	−0.503	−0.546	−0.531
q(O2)	−0.503	−0.486	−0.484

dx.doi.org/10.1021/jp301704n | J. Phys. Chem. A 2012, 116, 4510−4517

The calculated energies are presented in Table 2. A comparison of the total energies calculated at the CCSD(T)/aug-cc-pVTZ-PP level (ΔE + ΔZPVE) shows that the parallel structure is more stable than the linear structure by 2.20 kcal mol^{-1}. The MP2 calculations slightly overestimate this value whereas the DFT (B3LYP) method substantially underestimates it. A saturation of the basis set from triple-ζ (aug-cc-pVTZ-PP) to quadruple-ζ (aug-cc-pVQZ-PP) type was tested using the MP2 and DFT (B3LYP) methods, and an increase of the ΔE + ΔZPVE value by −0.53 kcal mol^{-1} was found for MP2. The interaction energy is negative for both structures at all computational levels meaning that their formation is accompanied by a decrease of the total energy. The interaction energy of the parallel structure is approximately three times greater than that of the linear structure at the CCSD(T)/aug-cc-pVTZ-PP level of theory.

Table 2. Energetic Parameters (in kcal mol^{-1}) for the HXeBr···CO_2 Complexes

basis set	aug-cc-pVTZ-PP			aug-cc-pVQZ-PP	
method	CCSD(T)	MP2	B3LYP	MP2	B3LYP
Relative Energy[a]					
	−2.20	−2.88	−1.01	−3.41	−1.01
Interaction Energy[b]					
parallel	−3.65	−3.85	−1.64	−4.11	−1.65
linear	−1.26	−1.84	−0.49	−3.05	−0.48

[a]Total energy difference ΔE between optimized geometrical structures of the parallel and linear complexes corrected by vibrational zero-point energy difference (ΔZPVE). [b]BSSE-corrected.

The vibrational frequencies are presented in Table 3. For the H−Xe stretching mode, the calculations give blue shifts for both parallel (+45.7 and +54.7 cm^{-1} at the MP2(full) and CCDS(T) levels, respectively) and linear (+75.1 and +103.4 cm^{-1}) structures. At both levels of theory, the blue shift for the parallel structure is smaller than that for the linear structure. This trend is in agreement with the charge redistribution in the molecule upon complex formation; i.e., the larger positive charge on the (HXe) part leads to an increase of the H−Xe stretching frequency.[8]

It is known that the harmonic frequencies of HNgY molecules deviate strongly from the experimental values.[6,22] We have estimated the anharmonic frequency of the H−Xe stretching mode using the harmonic frequency and the anharmonicity calculated for HXeBr by the correlation-corrected vibrational self-consistent field method.[39] The anharmonic frequencies obtained for the HXeBr monomer and two complex structures are presented in Table 4. For the monomer, the MP2 frequency including anharmonicity is still much larger than the experimental value whereas the CCSD(T) frequency including anharmonicity becomes close to the experimental value, especially in a neon matrix. The H−Xe stretching frequency shifts for the parallel and linear structures from the monomer are +50.3 and +94.8 cm^{-1} [CCSD(T)].

We also calculated the HBr···CO_2 complex, which is the principal precursor for the HXeBr···CO_2 complex. The calculations at the MP2(full) and CCSD(T) levels with the

Table 3. Calculated IR Spectra of HXeBr and CO_2 Monomers and HXeBr···CO_2 Complexes[a]

		HXeBr···CO_2 complexes			
mode	monomers HXeBr, CO_2	parallel	shift	linear	shift
		MP2(full)/ aug-cc-pVTZ-PP			
C═O asym stretch	2419.9 (554)	2420.2 (468)	+0.3	2421.2 (823)	+1.3
H−Xe stretch	1843.3 (1680)	1889.0 (1400)	+45.7	1918.3 (1037)	+75.1
C═O sym stretch	1335.9 (0)	1337.6 (1)	+1.8	1337.4 (2)	+1.6
OCO bend	667.1 (25)[b]	667.0 (20)	+2.9	665.9 (25)[b]	−1.2
		645.6 (51)	−21.4		
HXeBr bend	553.1 (3)[b]	549.0 (4)	−4.2	572.1 (4)[b]	+17.0
		544.9 (3)	−10.2		
Xe−Br stretch	196.5 (51)	191.5 (49)	−5.0	191.7 (65)	−4.8
intermolecular		103.5 (1)		41.0 (3)	
		64.9 (0)		27.2 (1)[b]	
		48.7 (5)		8.6 (3)[b]	
		29.5 (1)			
		CCSD(T)/ aug-cc-pVTZ-PP			
C═O asym stretch	2372.1	2369.9	+2.1	2373.2	+1.1
H−Xe stretch	1605.2	1659.8	+54.7	1708.6	+103.4
C═O sym stretch	1340.7	1339.7	−0.9	1341.7	+1.0
OCO bend	663.7[b]	663.2	−0.5	662.8[b]	−0.9
		643.4	−20.3		
HXeBr bend	527.2[b]	522.0	−5.17	534.5[b]	+7.4
		510.0	−17.2		
Xe−Br stretch	189.6	185.4	−4.2	185.6	−3.9
intermolecular		96.9		40.6	
		63.6		24.7[b]	
		39.0		3.2[b]	
		12.8			

[a]The calculated frequencies and shifts are in cm^{-1}, and IR intensities given in parentheses are in km mol^{-1}. The IR intensities are available only for MP2. [b]Degenerated vibrational modes.

dx.doi.org/10.1021/jp301704n | J. Phys. Chem. A 2012, 116, 4510−4517

Table 4. Calculated Harmonic and Anharmonic and Experimental Frequencies (in cm^{-1}) of the H−Xe Stretching Vibration of HXeBr Monomer and HXeBr···CO_2 Complexes[a,b,c]

	MP2		CCSD(T)		
	harmonic frequency[a]	anharmonic frequency[b]	harmonic frequency[a]	anharmonic frequency[b]	experiment in a xenon matrix
monomer	1843.3	1689.6	1605.2	1471.3	1504
parallel[c]	1889.0 (+45.7)	1731.4 (+41.8)	1659.8 (+54.7)	1521.4 (+50.3)	1557 (+52)
linear[c]	1918.3 (+75.1)	1758.3 (+68.7)	1708.6 (+103.4)	1566.1 (+94.8)	

[a]Harmonic frequencies are calculated with the aug-cc-pVTZ-PP basis set. [b]Anharmonic frequencies are obtained using the harmonic frequencies and computational anharmonicity reported in ref 39. [c]Frequency shifts from the monomer are shown in parentheses.

def2-TZVPPD basis set give two minima (Figure S1), in agreement with the previous reports.[40] The interaction energies for the linear and parallel forms are −1.40 and −1.20 kcal mol^{-1}, respectively [CCSD(T), BSSE corrected]. The vibrational frequencies calculated at the MP2(full) and CCSD(T) levels with the def2-TZVPPD basis set are presented in Table S1. The shifts of the HBr frequency are −7.7 and +0.2 cm^{-1} for the parallel and linear complexes at the CCSD(T)/def2-TZVPPD level of theory.

EXPERIMENTAL DETAILS AND RESULTS

The gaseous mixtures of HBr (≥99%, Aldrich), Xe (≥99.995%, AGA), and CO_2 (≥99.995%, AGA) were made by standard manometric procedures. The gas mixture ratios were HBr:CO_2:Xe = 1:(0−10):1000 and HBr:Xe:CO_2 = 1:(0−10):1000 for experiments in xenon and carbon dioxide matrices, respectively. These mixtures were deposited onto a CsI substrate in a close-cycle helium cryostat (DE 202A, APD). A xenon matrix containing DBr was prepared by passing the gaseous mixture of the HBr:Xe:CO_2 = 1:5:1000 mixture through a deposition line which contained a droplet of D_2SO_4. This method yielded up to 50% of the H/D exchange. The IR spectra (4000−400 cm^{-1}) were measured at 10 K using an FTIR spectrometer (Vertex 80v, Bruker) with 1 cm^{-1} resolution coadding 200 scans. The matrices were photolyzed with an excimer laser (MSX-250, MPB) operating at 193 nm (ArF). A low-pressure mercury lamp was also used to photolyze HXeBr molecules.

For an HBr/Xe matrix deposited at 30 K (Figure 2), monomeric HBr bands are observed at 2531.1 (strongest absorption, R branch), 2520 (Q branch), and 2508.9 cm^{-1} (P branch).[15] The amount of HBr dimer (2493.0 cm^{-1}) and trimer (2475.1 cm^{-1}) increases with the deposition temperature.[15] When CO_2 is added to the gas mixture, a CO_2-induced band appears around 2521.5 cm^{-1}. The other feature connected with the presence of CO_2 appears at 2529.2 cm^{-1} as a shoulder at the HBr monomeric band. Another less defined shoulder is seen on the blue side of the HBr monomeric band. These HBr···CO_2 bands are the strongest for deposition at 30 K and decrease in intensity as the deposition temperature becomes higher. Similar effects of the deposition temperature have been recently reported for the HBr···N_2 complex in a xenon matrix.[14]

Upon irradiation at 193 nm, HBr molecules dissociate to H and Br atoms. Bromine atoms are seen in the IR spectra at 3622 and 3648 cm^{-1} due to the spin−orbit transition ($^2P_{1/2} \leftarrow {}^2P_{3/2}$).[41] The progression of the $XeHXe^+$ absorptions is observed at 730.4, 842.3, 952.7, and 1061.6 cm^{-1}.[42] Annealing of photolyzed matrices at about 40 K mobilizes H atoms in a xenon matrix,[43] leading to the formation of HXeBr via the H + Xe + Br reaction of the neutral atoms.[1,2] The IR spectra in the H−Xe stretching region are shown in Figure 3. The HXeBr

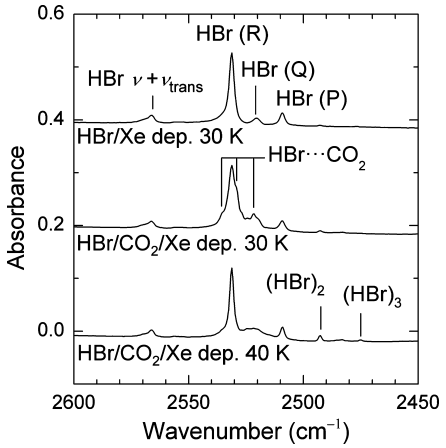

Figure 2. FTIR spectra in the HBr region measured (from top to bottom) for the HBr:Xe = 1:1000 sample deposited at 30 K and for the HBr:CO_2:Xe = 1:7:1000 sample deposited at 30 and 40 K. The $\nu + \nu_{trans}$ mode is the combination of the HBr stretching fundamental and the translational mode. The spectra were measured at 10 K.

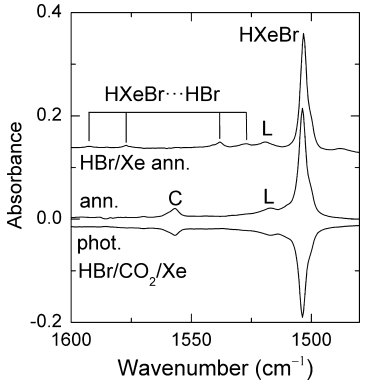

Figure 3. FTIR difference spectra showing (from top to bottom) the results of annealing at 40 K of the photolyzed HBr:Xe = 1:500 and HBr:CO_2:Xe = 1:7:1000 samples and of subsequent photolysis by 193 nm light of the annealed HBr:CO_2:Xe matrix. The negative bands in the lower spectrum show the decomposition of the species. The HXeBr···CO_2 complex band and HXeBr libration band are marked by C and L, respectively. The spectra were measured at 10 K.

monomer absorbs at 1504 cm^{-1}, and the satellite band at 1517 cm^{-1} (marked with L) originates from librational motion of monomeric HXeBr in a xenon matrix.[44] A number of bands of the HXeBr···HBr complex are also detected especially for higher HBr concentrations and deposition temperatures.[15] When CO_2 is added to the gas mixture, a new band at 1557 cm^{-1} (marked with C) appears in the spectrum after photolysis and annealing. This band is absent after deposition and photolysis, and it is observed only after annealing of photolyzed

dx.doi.org/10.1021/jp301704n | J. Phys. Chem. A 2012, 116, 4510−4517

xenon matrices containing simultaneously HBr and CO_2. The intensity of the 1557 cm^{-1} band relative to the HXeBr monomer band correlates well with the amount of CO_2 in the matrix. This band at 1557 cm^{-1} is assigned to the HXeBr···CO_2 complex in a xenon matrix. This species can be bleached efficiently by a short exposure to UV light similarly to the HXeBr monomers (lower trace in Figure 3). When the same gaseous mixture is deposited at a higher temperature of 40 K, the amount of the HXeBr···CO_2 complex becomes much smaller than for deposition at 30 K. For deposition at 50 K, the HXeBr···CO_2 complex is not formed, and instead, the HXeBr···HBr complexes rise. Similar trends at different deposition temperatures have been observed for the HXeBr···N_2 complex.[14]

In a carbon dioxide matrix, HBr molecule exhibits a single absorption band at 2549.5 cm^{-1} (lower trace in Figure 4),

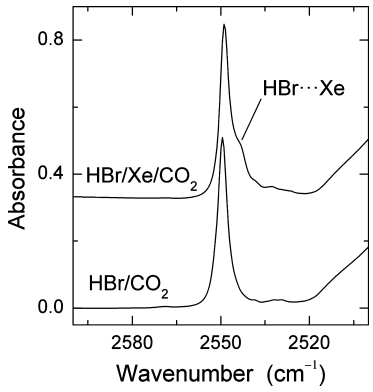

Figure 4. FTIR spectra in the HBr region measured for the HBr:Xe:CO_2 = 1:5:1000 (upper spectrum) and HBr:CO_2 = 1:1000 (lower spectrum) matrices. The spectra were measured at 10 K.

showing that it does not rotate similarly to HCl.[45] For the sample containing xenon, the monomer band is accompanied by a shoulder at about 2543 cm^{-1}. This shoulder most probably originates from the HBr···Xe complex, which will be the precursor for HXeBr in a carbon dioxide matrix. The 193 nm photolysis efficiently decomposes HBr. Annealing of a photolyzed HBr/Xe/CO_2 matrix at about 50 K leads to a new band at 1646 cm^{-1} (Figure 5). This band is absent after deposition and photolysis, and it is observed only after annealing of photolyzed carbon dioxide matrices containing simultaneously HBr and Xe. This band is easily decomposed by 193 nm light, and it is assigned to HXeBr in a carbon dioxide matrix. When we substituted HBr with HCl and/or Xe with Kr (see Figure 5), the corresponding band did not appear. In order to further support the assignment for HXeBr in a carbon dioxide matrix, we conducted experiments with DBr (Figure S2). The band corresponding to DXeBr in a carbon dioxide matrix appears at 1200 cm^{-1}, meaning the H/D frequency ratio of 1.372, which agrees well with the corresponding value for HXeBr in a xenon matrix (1.367).[3]

Figure 6a compares the stabilities of HXeBr and HXeBr···CO_2 in a xenon matrix and HXeBr in a carbon dioxide matrix measured at 60 K. At this temperature, a multimerization of HBr is not observed either in xenon or carbon dioxide matrices. In a xenon matrix, the HXeBr monomer decays faster than the HXeBr···CO_2 complex. The HXeBr monomer in a carbon dioxide matrix does not decay at 60 K. It has been checked that the decomposition of these

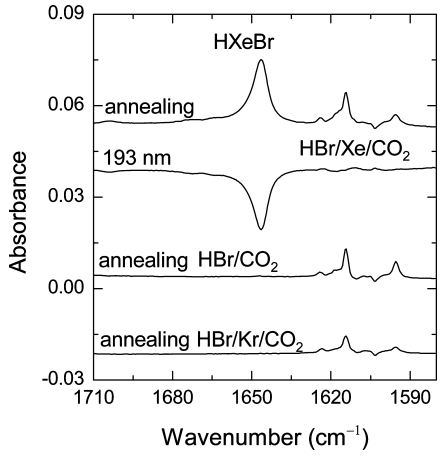

Figure 5. FTIR difference spectra in the H−Xe stretching frequency region showing (from top to bottom) the results of annealing of the photolyzed HBr:Xe:CO_2 = 1:5:1000 sample, the results of subsequent photolysis by 193 nm light of this annealed matrix, and the results of annealing of photolyzed HBr:CO_2 = 1:1000 and HBr:Kr:CO_2 = 1:5:1000 matrices. The negative bands in the second (from the top) spectrum show the decomposition of the species. Bands in the region between 1630 and 1590 cm^{-1} are due to H_2O in a carbon dioxide matrix. The samples were deposited at 40 K and annealed at 50 K for 5 min. The spectra were measured at 10 K.

species by the spectrometer Globar light is negligible. Figure 6b shows the relative concentrations of these species remaining

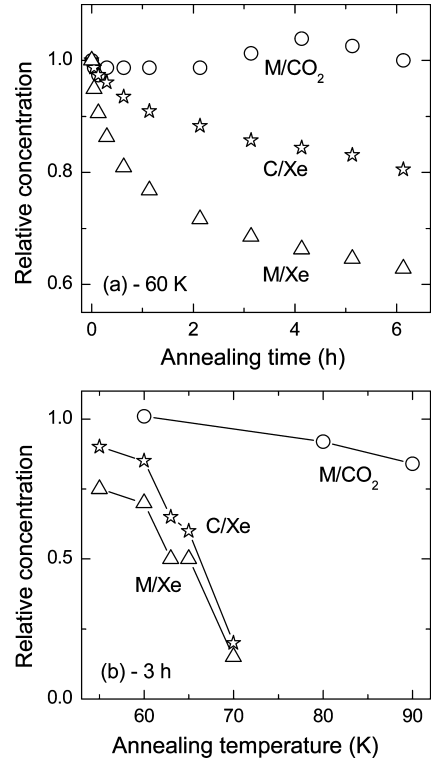

Figure 6. (a) Decay at 60 K of HXeBr monomer (M/Xe) and HXeBr···CO_2 complex (C/Xe) in a xenon matrix and of HXeBr in a carbon dioxide matrix (M/CO_2). (b) Proportion of the same species remaining after annealing for 3 h as a function of the annealing temperature. The relative concentrations were obtained by integrating the appropriate IR bands normalized by the value after first annealing at 50 K.

dx.doi.org/10.1021/jp301704n | J. Phys. Chem. A 2012, 116, 4510−4517

after 3 h of annealing at different temperatures. The decay of HXeBr and HXeBr···CO_2 in a xenon matrix is quite fast for annealing above 70 K whereas HXeBr in a carbon dioxide matrix is practically stable at this temperature. We were able to anneal a carbon dioxide matrix for a prolonged time at 100 K, and about 80% of HXeBr was present after 1 h of this annealing. When carbon dioxide matrices were annealed above 100 K, the matrices usually lost the contact with the CsI substrate and degraded fast.

DISCUSSION

HXeBr···CO_2 Complex. Figure 2 shows that the addition of CO_2 to the HBr/Xe mixture induces new bands in the HBr region. The two main bands can be assigned to the computationally predicted HBr···CO_2 complexes. The experimental frequency shifts from the Q transitions of the monomer are ca. +2 and +9 cm^{-1} for the bands at 2521.5 and 2529.2 cm^{-1}. These shifts seem to deviate from the computational shifts of −7.7 and +0.2 cm^{-1} for parallel and linear complexes, respectively. However, this difference is reasonable in a xenon matrix because the monomer-to-complex shift is influenced by the surrounding matrix atoms as discussed previously for the HBr···N_2 and HCl···N_2 complexes.[14] The smaller shoulder on the blue side of the monomeric band with a shift of about −3 cm^{-1} may be due to an additional matrix site.

The band observed at 1557 cm^{-1} for a photolyzed and annealed HBr/CO_2/Xe matrix is assigned to the HXeBr···CO_2 complex in solid xenon. This band is absent in the case of photolyzed and annealed HBr/Xe matrices. The intensity of the 1557 cm^{-1} band approximately correlates with the amount of the HBr···CO_2 complexes after matrix deposition when we change the CO_2 amount or deposition temperature. In other words, the HBr···CO_2 complex after deposition is the precursor for the HXeBr···CO_2 complex observed after photolysis and annealing. Upon photolysis, the HBr moiety of the HBr···CO_2 complex dissociates to H and Br atoms, and the H atom exits the cage. The Br···CO_2 complex participates in the annealing-induced reaction H + Xe + (Br···CO_2) to form the HXeBr···CO_2 complex. The 1557 cm^{-1} band appears synchronously with the 1504 cm^{-1} band of the HXeBr monomer at about 40 K, which corresponds to thermal mobilization of H atoms in solid xenon.[43] The complexation-induced blue shift (+53 cm^{-1}) is consistent with previous observations on HNgY complexes.[8] This assignment is supported by photobleaching the 1557 cm^{-1} band synchronously with the 1504 cm^{-1} band of the HXeBr monomer upon UV irradiation.

The structural assignment of the HXeBr···CO_2 complex is done on the basis of the computational results (Figure 1). The CCSD(T)/aug-cc-pVTZ-PP(Xe,Br) calculations predict blue shifts of +55 and +103 cm^{-1} for the parallel and linear complexes, respectively (+50 and +95 cm^{-1} after correction for anharmonicity). Experimentally, we observed only one band of the HXeBr···CO_2 complex blue-shifted from the monomer by +53 cm^{-1}, which fits better to the parallel complex. The calculated interaction energies confirm this assignment because the parallel structure is more stable than the linear structure by 2.20 kcal mol^{-1}. Moreover, interaction of HXeBr with CO_2 competes with its interaction with matrix atoms. The interaction energies of HXeBr···Xe are from −0.7 to −1.2 kcal mol^{-1} for different complexes obtained at the MP2/LJ18/6-311++G(2d,2p) level of theory.[44] Because these values are comparable with the interaction energy of the linear HXeBr···CO_2 complex (−1.26 kcal mol^{-1}), the formation of the linear HXeBr···CO_2 complex may be suppressed by the interaction of HXeBr with Xe atoms. Furthermore, it can be speculated that the parallel structure is more easily isolated in a matrix than the linear complex that occupies a larger volume. Finally, the two complexes have different precursors. In these experiments, we tried to maximize the HBr···CO_2 amount, which is the precursor for the parallel structure. The formation of the linear structure requires HBr and CO_2 molecules initially in different (adjacent) matrix cages, which may be an improbable event.

The blue shift of the H−Ng stretching frequency is a normal effect for the HNgY complexes because the $(HNg)^+Y^-$ ion-pair character is enhanced upon complexation.[8] It is interesting to compare the different 1:1 complexes of HXeBr. Among the experimentally observed complexes, the HXeBr···HBr complex has the largest shift of +148.9 cm^{-1}, and the HXeBr···HCl complexes show shifts from +84 to +121.5 cm^{-1}.[15] The large blue shifts in these complexes are probably due to a strong electrostatic effect between the dipoles, and the interaction between HXeBr and HBr is further enhanced due to the $(HXe)^+(BrHBr)^-$ character. Carbon dioxide has no permanent dipole moment, and the blue shift of the H−Xe stretching mode in the HXeBr···CO_2 complex is substantially smaller (+53 cm^{-1}). Even a smaller shift is observed for the HXeBr···N_2 complex (+11.5 and +16 cm^{-1}).[14] The calculated interaction energy is also substantially smaller for the HXeBr···N_2 complex than for HXeBr···CO_2. This difference may be attributed to the bigger quadrupole moment of CO_2 (−4.3 esu cm^2) compared to that of N_2 (−1.4 esu cm^2).[46] In accord, McDowell theoretically obtained a larger blue shift for the HArF···CO_2 complex (+217.5 cm^{-1}) than for the HArF···N_2 complex (+153 cm^{-1}).[47,48]

Next, we compare the HXeBr···CO_2 complex with the HXeCCH···CO_2 complex, which is the only HNgY···CO_2 complex observed experimentally to date. The H−Xe stretching bands of the HXeCCH···CO_2 complex are blue-shifted (+31.9 and +5.8 cm^{-1}) from the HXeCCH monomer in a xenon matrix.[16] The parallel structure is the most stable in both HXeBr···CO_2 and HXeCCH···CO_2 complexes having similar interaction energies. However, the calculated shift is more than twice larger for the HXeBr···CO_2 complex; thus, the agreement between experiment and theory is reasonable.

HXeBr in a Carbon Dioxide Matrix. Figure 4 shows that the addition of xenon to the HBr/CO_2 mixture induces a new band at 2543 cm^{-1} in the HBr region. This band is assigned to the HBr···Xe complex, which is the precursor for HXeBr in a carbon dioxide matrix. The same procedure worked for the preparation of some noble-gas hydrides in other noble-gas matrices, for example, HXeBr in a neon matrix.[24] The 193 nm radiation decomposes HBr in the HBr···Xe compex. The H atoms are mobilized by annealing above 40 K, reacting with BrXe centers to form HXeBr molecules with the absorption at 1646 cm^{-1}. The 1646 cm^{-1} band is not observed in the experiments with HBr/CO_2 and HBr/Kr/CO_2 matrices, indicating that this band is truly xenon-induced. DXeBr is observed at 1200 cm^{-1}, meaning the ν(H−Xe)/ν(D−Xe) ratio of 1.372. This deuteration effect agrees with that obtained for HXeBr in a xenon matrix, confirming the assignment for HXeBr in a carbon dioxide matrix.

The H−Xe stretching frequency of HXeBr is 1504, 1524, 1452, and 1646 cm^{-1} in xenon, krypton, neon, and carbon dioxide matrices, respectively. It is believed that the frequency

dx.doi.org/10.1021/jp301704n | J. Phys. Chem. A 2012, 116, 4510−4517

in a neon matrix is close to the hypothetical gas-phase value. The H−Xe stretching mode is shifted by +52, +72, and +196 cm^{-1} in xenon, krypton, and carbon dioxide matrices relative to a neon matrix, respectively. The big difference in the H−Xe stretching frequency between neon and carbon dioxide matrices suggests that the H−Xe bond of HXeBr in a carbon dioxide matrix is about 30% stronger, in terms of the force constant than that in a neon matrix. The smallest frequency in a neon matrix is consistent with the concept of the normal case of blue-shifting bonds for the HNgY molecules.[8] From this viewpoint, the higher frequency in a krypton matrix compared to a xenon matrix looks rather strange because the interaction with xenon should be stronger. Tanskanen et al. attempted to explain the matrix-induced shifts for HXeCCH in argon, krypton, and xenon matrices where the H−Xe stretching frequencies were $\nu(Ar) > \nu(Kr) > \nu(Xe)$.[49] They calculated the frequency shifts for the 1:1 complexes HXeCCH···Ng (Ng = Ar, Kr, and Xe); however, these calculations could not explain the experimental results. It was concluded that bigger HXeCCH@Ng_n systems should be studied for adequate description of the experiment. The same is presumably valid for the case of a carbon dioxide matrix.

Thermal Stability. Figure 6 shows a strong effect of carbon dioxide molecules on the thermal stability of HXeBr. At 60 K, the HXeBr···CO_2 complex in a xenon matrix decays more slowly than the HXeBr monomer in a xenon matrix whereas the HXeBr monomer in a carbon dioxide matrix does not decay at all. The difference in thermal stabilities of HXeBr and HXeBr···CO_2 in a xenon matrix is not substantial for annealing at 70 K, especially taking into account that additional complexes can be formed upon thermal mobilization of molecules.[17] The strong stabilization effect observed in a carbon dioxide matrix is more remarkable. For annealing above 70 K, the difference between stabilities of HXeBr in xenon and carbon dioxide matrices becomes dramatic. Several aspects of this finding should be considered. First, the different stability can originate from a change of decomposition barriers upon interaction with the carbon dioxide matrix compared to xenon. Second, the matrix becomes less rigid at elevated temperatures, and the sublimation temperature is higher for carbon dioxide than for xenon, which makes a difference in mobility of species in the matrices. In the latter case, the mobility of lattice vacancies may be important.[10] Finally, there may be a destabilization effect of a xenon matrix, which is smaller in a carbon dioxide matrix. For example, a process

$$Xe\cdots(HXe)^+Br^- \rightarrow (XeHXe)^+\cdots Br^- \quad (3)$$

may be operating to some extent; however, its barrier has not been studied.

The observed thermal stability correlates with the H−Xe stretching frequency that is 1504 cm^{-1} for the HXeBr monomer in a xenon matrix, 1557 cm^{-1} for the HXeBr···CO_2 complex in a xenon matrix, and 1646 cm^{-1} for the HXeBr monomer in a carbon dioxide matrix. One may speculate that the observed stabilization effect is a consequence of the strengthening of the H−Xe bond. However, this interpretation is not straightforward. Indeed, the surrounding molecules can in general stabilize or destabilize the HNgY molecules as it has been theoretically shown for HXeOH in a small water cluster.[18] The surrounding water molecules strengthen the H−Xe bond of HXeOH, resulting in stabilization with respect to the 3B channel; however, they decrease the bending barrier, which leads to the decomposition of the molecule.[18] This is obviously not the case for HXeBr in a carbon dioxide matrix where HXeBr is relatively stable above the cryogenic limit (at least up to 100 K). Further studies should reveal whether this conclusion is valid for all noble-gas hydrides or not. In the present series of experiments, we have tried to prepare HXeCl and HXeCCH in a carbon dioxide matrix; however, our attempts have failed.

It is not clear whether 2B or 3B channel is more important in the thermal decay of HXeBr because there has not been a theoretical study on the decomposition channels of HXeBr especially when interacting with the matrix. The calculations performed for HNgY species in vacuum disagree with the experimental results obtained in matrices in the case of HXeOH and HXeOXeH.[23] The present results may indicate that HXeBr dissociates preferentially via 3B channel so that the strengthening of the H−Xe bond stabilizes the molecule, and the possible decrease of the bending barrier is not substantial. In order to explain the huge difference in stability of HXeBr in xenon and carbon dioxide matrices, theoretical studies on dissociation channels and barriers of HXeBr in xenon and carbon dioxide clusters are needed, and this is a challenge for future theoretical studies.

CONCLUSIONS

We have prepared the HXeBr···CO_2 complex in a xenon matrix and characterized it by IR absorption spectroscopy. The complex was made by photolysis of the HBr···CO_2 complex trapped in a xenon matrix and subsequent thermal mobilization of the H atom. The H−Xe stretching absorption of the HXeBr···CO_2 complex was observed at 1557 cm^{-1}, blue-shifted by +53 cm^{-1} from the HXeBr monomer. Two structures (parallel and linear) were found computationally for the HXeBr···CO_2 complex, the parallel structure being more stable (interaction energy −3.65 kcal mol^{-1} at the best level of theory used here). The harmonic H−Xe stretching mode is blue-shifted by +55 and +103 cm^{-1} for parallel and linear structures, respectively. On the basis of the interaction energy and the frequency shifts, the experimentally observed band is assigned to the parallel structure. The spectral shift of the HXeBr···CO_2 complex (+53 cm^{-1}) is larger than that of HXeBr···N_2 (+11.5 and +16 cm^{-1}),[14] indicating that quadrupole moments play an important role in stabilizing the H−Ng bond. On the other hand, the HXeBr···HBr complex has a bigger interaction energy (up to about −7 kcal mol^{-1}) and the H−Xe stretching frequency shift (up to +150 cm^{-1}).[15]

An important result of the present work is the preparation and identification of HXeBr in carbon dioxide ice. This is the first observation of a noble-gas hydride in a molecular solid. DXeBr was also prepared to confirm the assignment. The H−Xe stretching frequencies of HXeBr and DXeBr in a carbon dioxide matrix are 1646 and 1200 cm^{-1}, respectively. The $\nu(H-Xe)/\nu(D-Xe)$ ratio of 1.372 agrees well with the previous results on noble-gas hydrides. The large matrix-induced shift between carbon dioxide and neon matrices (~200 cm^{-1}) indicates a strong stabilization of the H−Xe bond by carbon dioxide molecules.

The most striking observation of this work is the efficient stabilization of HXeBr molecule by carbon dioxide ice as compared to a xenon matrix. This is directly evidenced by the experiments with thermal annealing, where HXeBr in a xenon matrix decays much faster than HXeBr in a carbon dioxide matrix. HXeBr in a carbon dioxide matrix is relatively stable

well above the cryogenic limit (at least up to 100 K), i.e., under conditions that may occur in nature.

■ ASSOCIATED CONTENT

Supporting Information

Calculated structures (Figure S1) and vibrational frequencies (Table S1) of the HBr···CO_2 complexes and the spectra of DBr and DXeBr in a carbon dioxide matrix (Figure S2). This material is available free of charge via the Internet at http://pubs.acs.org.

■ AUTHOR INFORMATION

Corresponding Author

*E-mail: leonid.khriachtchev@helsinki.fi.

Notes

The authors declare no competing financial interest.

■ ACKNOWLEDGMENTS

The work was supported by the Finnish Centre of Excellence in Computational Molecular Science and by the Academy of Finland (Grant 139105). S.B. and Z.L. acknowledge the National Center for Research and Development of Poland for the support of this research (Grant ERA-CHEMISTRY-2009/01/2010). The authors thank the Wroclaw Centre for Networking and Supercomputing for generous allocation of computer time.

■ REFERENCES

(1) Khriachtchev, L.; Räsänen, M.; Gerber, R. B. *Acc. Chem. Res.* **2009**, *42*, 183−191.
(2) Grochala, W.; Khriachtchev, L.; Räsänen, M. In *Physics and Chemistry at Low Temperatures*; Khriachtchev, L., Ed.; Pan Stanford Publishing: Singapore, 2011; pp 51−84.
(3) Pettersson, M.; Lundell, J.; Räsänen, M. *J. Chem. Phys.* **1995**, *102*, 6423−6431.
(4) Khriachtchev, L.; Pettersson, M.; Runeberg, N.; Lundell, J.; Räsänen, M. *Nature* **2000**, *406*, 874−876.
(5) Khriachtchev, L.; Pettersson, M.; Lignell, A.; Räsänen, M. *J. Am. Chem. Soc.* **2001**, *123*, 8610−8611.
(6) Khriachtchev, L.; Tapio, S.; Domanskaya, A. V.; Räsänen, M.; Isokoski, K.; Lundell, J. *J. Chem. Phys.* **2011**, *134*, 124307.
(7) McDowell, S. A. C. *Curr. Org. Chem.* **2006**, *10*, 791−803.
(8) Lignell, A.; Khriachtchev, L. *J. Mol. Struct.* **2008**, *889*, 1−11.
(9) Bochenkova, A. V.; Khriachtchev, L.; Lignell, A.; Räsänen, M.; Lignell, H.; Granovsky, A. A.; Nemukhin, A. V. *Phys. Rev. B* **2008**, *77*, 094301.
(10) Bochenkova, A. V.; Bochenkov, V. E.; Khriachtchev, L. *J. Phys. Chem. A* **2009**, *113*, 7654−7659.
(11) Lignell, A.; Khriachtchev, L.; Pettersson, M.; Räsänen, M. *J. Chem. Phys.* **2002**, *117*, 961−964.
(12) Lignell, A.; Khriachtchev, L.; Pettersson, M.; Räsänen, M. *J. Chem. Phys.* **2003**, *118*, 11120−11128.
(13) Corani, A.; Domanskaya, A.; Khriachtchev, L.; Räsänen, M.; Lignell, A. *J. Phys. Chem. A* **2009**, *113*, 10687−10692.
(14) Khriachtchev, L.; Tapio, S.; Räsänen, M.; Domanskaya, A.; Lignell, A. *J. Chem. Phys.* **2010**, *133*, 084309.
(15) Lignell, A.; Lundell, J.; Khriachtchev, L.; Räsänen, M. *J. Phys. Chem. A* **2008**, *112*, 5486−5494.
(16) Tanskanen, H.; Johanson, S.; Lignell, A.; Khriachtchev, L.; Räsänen, M. *J. Chem. Phys.* **2007**, *127*, 154313.
(17) Domanskaya, A.; Kobzarenko, A. V.; Tsivion, E.; Khriachtchev, L.; Feldman, V. I.; Gerber, R. B.; Räsänen, M. *Chem. Phys. Lett.* **2009**, *481*, 83−87.
(18) Nemukhin, A. V.; Grigorenko, B. L.; Khriachtchev, L.; Tanskanen, H.; Pettersson, M.; Räsänen, M. *J. Am. Chem. Soc.* **2002**, *124*, 10706−10711.
(19) Khriachtchev, L.; Tanskanen, H.; Pettersson, M.; Räsänen, M.; Ahokas, J.; Kunttu, H.; Feldman, V. *J. Chem. Phys.* **2002**, *116*, 5649−5656.
(20) Tsivion, E.; Zilberg, S.; Gerber, R. B. *Chem. Phys. Lett.* **2008**, *460*, 23−26.
(21) Tsivion, E.; Gerber, R. B. *Phys. Chem. Chem. Phys.* **2011**, *13*, 19601−19606.
(22) Khriachtchev, L.; Isokoski, K.; Cohen, A.; Räsänen, M.; Gerber, R. B. *J. Am. Chem. Soc.* **2008**, *130*, 6114−6118.
(23) Tsivion, E.; Gerber, R. B. *Chem. Phys. Lett.* **2009**, *482*, 30−33.
(24) Lorenz, M.; Räsänen, M.; Bondybey, V. E. *J. Phys. Chem. A* **2000**, *104*, 3770−3774.
(25) Tielens, A. G. G. M.; Allamandola, L. J. In *Physics and Chemistry at Low Temperatures*; Khriachtchev, L., Ed.; Pan Stanford Publishing: Singapore, 2011; pp 341−380.
(26) Pople, J. A.; Head-Gordon, M.; Raghavachari, K. *J. Chem. Phys.* **1987**, *87*, 5968−5975.
(27) Møller, C.; Plesset, M. S. *Phys. Rev.* **1934**, *46*, 618−622.
(28) Becke, A. D. *J. Chem. Phys.* **1993**, *98*, 1372−1377.
(29) Becke, A. D. *J. Chem. Phys.* **1993**, *98*, 5648−5652.
(30) Lee, C.; Yang, W.; Parr, R. G. *Phys. Rev. B* **1988**, *37*, 785−789.
(31) Dunning, T. H., Jr. *J. Chem. Phys.* **1989**, *90*, 1007−1023.
(32) Kendall, R. A.; Dunning, T. H., Jr.; Harrison, R. J. *J. Chem. Phys.* **1992**, *96*, 6796−6806.
(33) Feller, D. *J. Comput. Chem.* **1996**, *17*, 1571−1586.
(34) Schuchardt, K. L.; Didier, B. T.; Elsethagen, T.; Sun, L.; Gurumoorthi, V.; Chase, J.; Li, J.; Windus, T. L. *J. Chem. Inf. Model.* **2007**, *47*, 1045−1052.
(35) Boys, S. F.; Bernardi, F. *Mol. Phys.* **1970**, *19*, 553−566.
(36) Weinhold, F. In *Encyclopedia of Computational Chemistry*, 1st ed.; Wiley & Sons: New York, 1998, pp 1792−1811.
(37) Werner, H.-J.; Knowles, P. J.; Manby, F. R.; Schütz, M.; Celani, P.; Knizia, G.; Korona, T.; Lindh, R., Mitrushenkov, A.; Rauhut, G.; et al. *Molpro, Version 2010.1*; University of Birmingham: Birmingham, U.K., 2010.
(38) Frisch, M. J.; Trucks, G. W.; Schlegel, H. B.; Scuseria, G. E.; Robb, M. A.; Cheeseman, J. R.; Scalmani, G.; Barone, V.; Mennucci, B.; Petersson, G. A.; et al. *Gaussian 09, Revision B.01*; Gaussian Inc.: Wallingford, CT, 2009.
(39) Lundell, J.; Chaban, G. M.; Gerber, R. B. *J. Phys. Chem. A* **2000**, *104*, 7944−7949.
(40) Zeng, Y. P.; Sharpe, S. W.; Shin, S. K.; Wittig, C.; Beaudet, R. A. *J. Chem. Phys.* **1992**, *97*, 5392−5402 and references therein.
(41) Pettersson, M.; Nieminen, J. *Chem. Phys. Lett.* **1998**, *283*, 1−6.
(42) Kunttu, H.; Seetula, J.; Räsänen, M.; Apkarian, V. A. *J. Chem. Phys.* **1992**, *96*, 5630−5635.
(43) Khriachtchev, L.; Tanskanen, H.; Pettersson, M.; Räsänen, M.; Feldman, V.; Sukhov, F.; Orlov, A.; Shestakov, A. F. *J. Chem. Phys.* **2002**, *116*, 5708−5716.
(44) Khriachtchev, L.; Lignell, A.; Juselius, J.; Räsänen, M.; Savchenko, E. *J. Chem. Phys.* **2005**, *122*, 014510.
(45) Barnes, A. J.; Hallam, H. E.; Scrimshaw, G. F. *Trans. Faraday Soc.* **1969**, *65*, 3159−3171.
(46) Buckingham, A. D.; Disch, R. L.; Dunmur, D. A. *J. Am. Chem. Soc.* **1968**, *90*, 3104−3107.
(47) McDowell, S. A. C. *Phys. Chem. Chem. Phys.* **2003**, *5*, 808−811.
(48) McDowell, S. A. C. *Chem. Phys. Lett.* **2005**, *406*, 228−231.
(49) Tanskanen, H.; Khriachtchev, L.; Lundell, J.; Räsänen, M. *J. Chem. Phys.* **2006**, *125*, 074501.